Protein Nanopatterns for Improved Immunodetection Sensitivity

ARTICLE *in* ANALYTICAL CHEMISTRY · SEPTEMBER 2008

Impact Factor: 5.64 · DOI: 10.1021/ac801021z · Source: PubMed

Anal. Chem. **2008,** *80,* 7336–7340

Protein Nanopatterns for Improved Immunodetection Sensitivity

A. Valsesia,* I. Mannelli, P. Colpo, F. Bretagnol, and F. Rossi

European Commission, Joint Research Centre, Institute for Health and Consumer Protection, 21020 Ispra (VA), Italy

In this work, we clearly demonstrate the capability of protein nanopatterns of improving the quality factors of immunosensing devices, such as lowering of the limit of detection and increase of sensitivity. This beneficial effect is obtained by the formation on the sensor's surface of bioadhesive domains of nanometric dimensions in a nonadhesive matrix by means of colloidal lithography.

Biosensors play a very important role for the development of point-of-care analysis thanks to their interesting characteristics such as rapid and sensitive detection capabilities.[1−4]

As a consequence, a constant effort is made by researchers in order to improve their performance in terms of sensitivity and specificity. Among others, the control of the interface between the transducer and the biological probes is a crucial issue since the biointerface is the essential element that guaranties the bioactivity of the immobilized biological probes.[5] The control of the biointerface is typically addressed by functionalizing the surface with chemical groups that interact properly with the proteins immobilized.[6−9] Besides, new nanobiotechnology-based tools have led to more sophisticated approaches that use, for instance, nanostructured surfaces.[10] Nanostructures can have typical dimensions on the order of magnitude of those of proteins (from a few nanometers to tens of nanometers) so that they are able to interact on the same critical length scale. Benefits have been already shown in many publications in terms of densification of protein nanoarrays[11] and as well in terms of the improvement of immunoreaction efficiency.[12,13]

In the present work, we study, by means of a quartz crystal microbalance (QCM), the bioactivity properties of antibodies immobilized on nanostructured biointerfaces composed of adhesive nanodomains surrounded by an antiadhesive matrix. In our previous work, we have demonstrated that such nanopatterned interfaces induce the confined adsorption of proteins within the adhesive areas leading to an increment in the immunoreaction efficiency.[14] In this work, we show for the first time that the use of the nanostructured surfaces results in the improvement of the limit of detection of the immunosensor with respect to a homogeneously functionalized surface.

EXPERIMENTAL SECTION

Fabrication of the Nanostructures. The nanostructured surfaces are composed of two plasma polymers, one being bioactive with carboxylic function (poly(acrylic acid)) and the other one an antiadhesive (poly(ethylene oxide)). The nanopatterning is fabricated by using nanosphere lithography.

Plasma polymerized acrylic acid films (ppAA) and poly(ethylene oxide) (PEO-like) films are deposited in two separated reactors, using a glow discharge created from acrylic acid and DEGDME vapors, respectively. Further details are given in previous work.[15]

Polystyrene (PS) beads used for nanosphere lithography (diameter of 200, 500m and 1000 nm, Sigma-Aldrich) are negatively charged stabilized colloidal particles with a nominal size dispersion factor of 10%. Oxygen plasma etching is carried out in an inductively coupled plasma source, a high-density plasma source already described in ref 16.

The process of fabrication of the nanostructures is described in Figure 1a−d and the respective SEM characterization pictures for each fabrication step are shown in Figure 1e−h. The processing steps for the production of the nanostructured surfaces are the following: first, a ppAA layer, rich in COOH functionalities (COOH density of 7 groups/nm^2) is deposited on the quartz crystal. Etching of the ppAA film is performed through a mask made from a 2D crystal formed by PS beads (Figure 1a and e). The formation of the nanomask is carried out according to the following procedure: first a microdrop (drop volume, 5 μL) of PS beads suspension (nominal colloidal concentration 2% of solid content) is deposited on the ppAA functionalized quartz crystal surface with the spin-coater off. The sample is then spun at an optimized speed favoring the slow evaporation of the liquid, in order to allow the organization of the PS beads in a hexagonal crystal lattice. By adjusting the spinning acceleration, it is possible

* To whom correspondence should be addressed. E-mail: andrea.valsesia@jrc.it.

(1) Rogers, K. R. *Appl. Biochem. Biotechnol., Part B: Mol. Biotechnol.* **2000**, *14*, 109–129.
(2) Collings, A. F.; Caruso, F. *Rep. Prog. Phys.* **1997**, *60*, 1397–1445.
(3) Dong, S.; Chen, X. *Rev. Mol. Biotechnol.* **2002**, *82*, 303–323.
(4) Luppa, P. B.; Sokoll, L. J.; Chan, D. W. *Clin. Chim. Acta* **2001**, *314*, 1–26.
(5) Kasemo, B. *Curr. Opin. Solid State Mater. Sci.* **1998**, *3*, 451–459.
(6) Horbett, T. A. *Surfactant Sci. Ser.* **2003**, *110*, 393–413.
(7) Hlady, V.; Buijs, J. *Cur. Opin. Biotechnol.* **1996**, *7*, 72–77.
(8) Dee, K. C.; Puleo, D. A.; Bizios, R. *Introduction Tissue-Biomater. Interact.* **2002**, 37–52.
(9) Szleifer, I. *Biophys. J.* **1997**, *72*, 595–612.
(10) Haes, A. J.; Zou, S.; Schatz, G. C.; Duyne, R. P. V. *J. Phys. Chem. B* **2004**, *108*, 109–116.
(11) Lee, K. B.; Kim, E. Y.; Mirkin, C. A.; Wolinsky, S. M. *Nano Lett.* **2004**, *4*, 1869–1872.
(12) Agheli, H.; Malmstroem, J.; Larsson, E. M.; Textor, M.; Sutherland, D. S. *Nano Lett.* **2006**, *6*, 1165–1171.
(13) Valsesia, A.; Colpo, P.; Meziani, T.; Lisboa, P.; Lejeune, M.; Rossi, F. *Langmuir* **2006**, *22*, 1763–1767.
(14) Valsesia, A.; Colpo, P.; Mannelli, I.; Mornet, S.; Bretagnol, F.; Ceccone, G.; Rossi, F. *Anal. Chem.* **2008**, *80*, 1418–1424.
(15) Valsesia, A.; Silvan, M. M.; Ceccone, G.; Gilliland, D.; Colpo, P.; Rossi, F. *Plasma Processes Polym.* **2005**, *2*, 334–339.

10.1021/ac801021z CCC: $40.75
Published on Web 08/19/2008

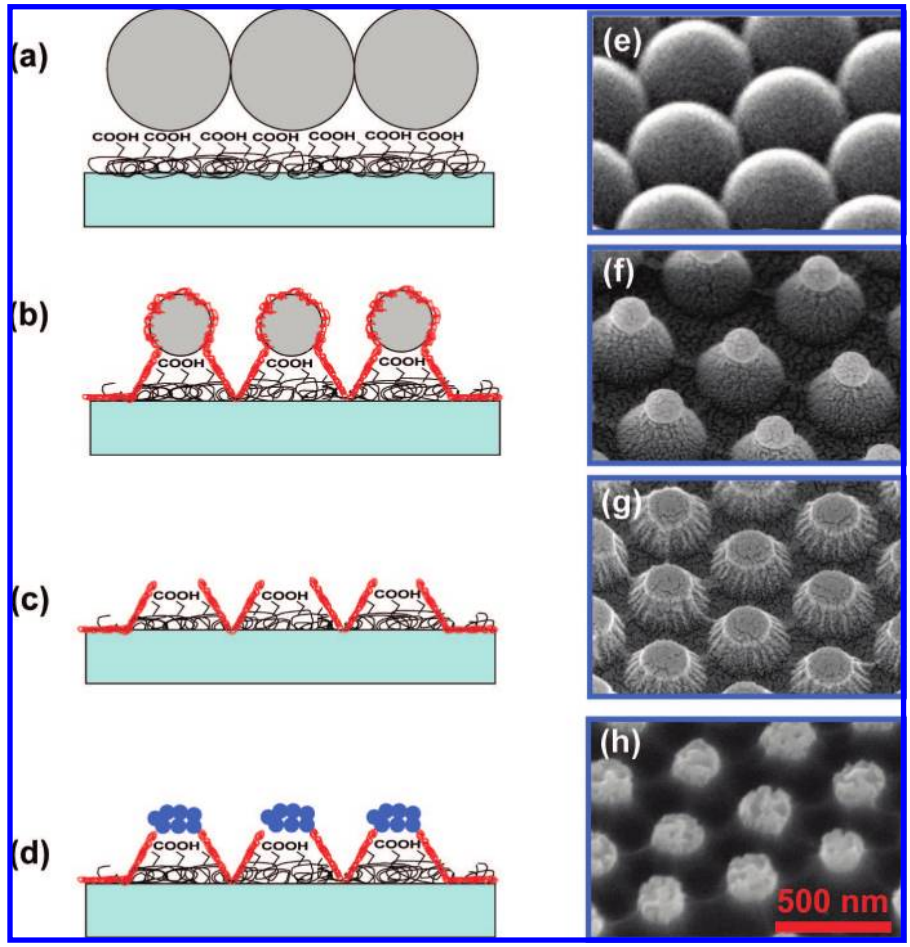

Figure 1. (a)−(d) Description of the nanofabrication process. (e)−(h) SEM characterization of each processing step.

to create macroscopic homogeneous areas covered by monolayered nanobeads of few square millimeters with a surface coverage ranging from 70 to 100%.

The nanomask pattern is then transferred to the ppAA layer by means of oxygen plasma etching (Figure 1b and f). Atomic oxygen free radicals produced in the plasma discharge are recognized to initiate the etching process by different mechanisms involving chemical reactions of the oxygen atoms with the alkyl chains of the polymers, their functional groups, or both.[17]

SEM analysis of the etched sample (Figure 1f) reveals that the plasma etches the particles and creates conical nanostructures in the ppAA layer.

The etching operation has to be accurately controlled in order to create the nanostructures on the ppAA layer and avoid PS mask over etching. Once the nanostructures are created in the ppAA film, a thin layer (<10 nm) of PEO-like is deposited by PE-CVD (this is described by the red layer in Figure 1). The morphology of the surface is unchanged with respect to the previous step.

The last step consists in removing the etched nanobeads from the surface by an ultrasonic bath in water for 5 min. The surface is finally characterized by bioadhesive COOH spots separated by nonadhesive PEO-like coating (Figure 1c and g).

As a proof of concept, we exposed the nanopatterned surface to 20 μg/mL BSA solution. After washing and drying, the sample surface was characterized by SEM, and the result is shown in Figure 1h: the proteins stick selectively on the adhesive COOH spots leaving the PEO-like matrix free of proteins Figure 1d and h). From the SEM images, we can also estimate the size of the adhesive COOH areas: these are ~100 nm wide, covering ~5% of the total sensing area. Several nanopatterned surfaces have been fabricated by using nanobeads of 200, 500, and 1000 nm in diameter. Etching time has been adjusted in order to have a similar active area for the three surfaces.

Table 1. Geometric Parameters for the Three Different Nanopatterned Surfaces[a]

sample	COOH-spot diameter (2 L) (nm)	lattice constant (d, nm)	number of spots (N_{ND})	total COOH functionalized area (nm^2)
ppAA				2×10^{13}
ND200	50	200	5.8×10^8	$\sim 1 \times 10^{12}$
ND500	100	500	9.2×10^7	$\sim 1 \times 10^{12}$
ND1000	200	1000	2.3×10^7	$\sim 1 \times 10^{12}$

[a] In the acronym of the samples' name, ND stands for Nano Dome, while the number refers to the lattice constant of the colloidal mask.

The geometric characteristics of the different nanopatterned surfaces are summarized in Table 1. The 5 μm × 5 μm AFM scans for the three nanopatterned surfaces are shown in Figure 2.

Those geometrical parameters have been calculated by considering an active area of the crystal of A_{act} = 0.2 cm^2 = 2×10^{13} nm^2.

(16) Meziani, T.; Colpo, P.; Rossi, F. *Plasma Sources Sci. Technol.* **2001**, *10*, 276–283.
(17) Egitto, F. *Pure Appl. Chem.* **1990**, *62*, 1699–1708.

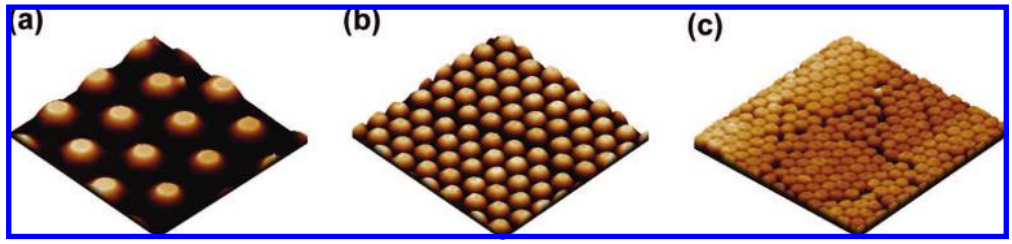

Figure 2. The 5 μm $\times$ 5 μm AFM scan of (a) ND1000, (b) ND500, and (c) ND200 surfaces. Vertical scale is [0;60 nm].

QCM-D Measurements. Quartz crystal microbalance with dissipation (QCM-D) (Qsense, Sweden) has been used for quantitatively measuring the mass of proteins absorbed on uniformly functionalized and nanostructured surfaces.

The measurement procedure used in this study is the following: both the probe (human IgG) immobilization and the antibody/antigen interactions (human IgG/anti-human IgG) have been monitored online. The nanopatterned quartz resonator was held in the measurement cell, and the baseline was recorded when the carrier buffer (phosphate-buffered saline (PBS): 10 mM PBS, pH 7.4) was flowing in the reaction cell. For the probe immobilization, human IgGs with concentration of 5 μg/mL in PBS solution was injected in the liquid cell. The adsorption was monitored overnight.

Before the antibody/antigen interaction monitoring, the specificity of the system was assessed by flowing in the reaction cell a 20 μg/mL monoclonal anti-chicken egg albumin (Ab-OVA) in PBS solution. After the rinsing with PBS, the anti-human IgG Fab specific at various concentrations (Ab-IgG) was injected until signal stabilization and a final rinsing of the surface was performed, to remove loosely bound biomolecules. The results are expressed as the difference between the frequency shift values measured after the rinsing step and before the sample injection. The same buffer solution was used for all the experiments.

All the proteins were purchased from Sigma-Aldrich: human IgG, purified immunoglobulin (code I2511), albumin from bovine serum (BSA) (code A4503), monoclonal anti-chicken egg albumin, clone OVA-14, mouse ascites fluid (Ab-OVA) (code A6075), anti-human IgG, Fab specific, and affinity isolated antigen specific antibody (Ab-IgG) (code I5260). PBS tablets were from Sigma-Aldrich.

RESULTS AND DISCUSSION

The immunoreactivity of the IgG molecules immobilized on the different surfaces has been determined by exposing the surfaces to Ab-IgG solutions with different concentrations, enabling the construction of the dose−response curves for the present immunosensor for the four types of surfaces. These curves for the different surfaces tested are shown in Figure 3.

In the case of nanostructures, the areas covered by PEO-like are considered totally protein repellent since the measurement by QCM did not show detectable protein adsorption on PEO-like layers.[18]

Figure 3 shows that the curves corresponding to ND500 and ND200 are shifted to the lower concentration range demonstrating that nanostructuring the surface improves the limit and the sensitivity of detection. From these curves, two regimes are distinguishable in the case of both the ND200 and the ND500 surfaces: (1) For Ab-Ig concentration of >0.3 μg/mL (black region in Figure 3a−c), the absolute amount of antibodies detected is higher for the homogeneous ppAA surface. (2) For Ab-Ig concentration of <0.3 μg/mL (red region in Figure 3a,b), the binding capacity of the nanostructured surface is higher than on the ppAA surface, leading to a decrease of the limit of detection.

The ND1000 surface does not show any evidence of the limit of detection improvement.

The calibration curves were fitted with a sigmoidal-shaped function, which is commonly used for ligand binding assays.[19] The fitting function used is

$$\Delta F(C) = \mathrm{A2} + (\mathrm{A1} - \mathrm{A2})/(1 + C/C_0)^p \qquad (1)$$

where A2 is the saturation value and C_0 is the analyte concentration that gives the half of the value obtained at saturation. C_0 is the concentration placed in the middle of the region of concentrations at which the sensor response is linear; hence, the lower the C_0 the lower the working region of concentration of the sensor. The slope factor p is the slope of the curve in the linear region and is a measurement of the sensitivity (variation of signal as a function of the variation of concentration). A1 is the saturation value corresponding to the zero concentration, which is typically zero.

The limit of detection (LOD) for the different surfaces has been calculated as the minimum concentration of the Ab-IgG that gave a measurable signal (>3N, where N is the root mean square value of the noise, typically for a Q-sense measurement 3N is 0.15 Hz). The fitted parameters for the calibration curves for the different surfaces are reported in Table 2.

From the fitted values of table, we can observe:

(1) The saturation A2 is almost 10 times larger for the ppAA surface than for the nanostructured, as expected, due to a larger ppAA active area as compared to the nanostructured surfaces (see Table 1).

(2) The sensitivity p is larger on the nanostructured surface than on the ppAA surface.

(3) C_0 concentration, i.e., the working region, is in the lower concentration range for the nanostructured surfaces as compared to the unstructured ppAA. The reduction is meaningful on the ND200 and ND500 surfaces and corresponds to a factor 7. On the ND1000 surface, the fitted C_0 value is not significantly different from the ppAA surface.

The reduction of C_0 on the nanostructured surfaces is reflected also in a reduction of the LOD of a factor of 5 with

(18) Belegrinou, S.; Mannelli, I.; Lisboa, P.; Bretagnol, F.; Valsesia, A.; Ceccone, G.; Colpo, P.; Rauscher, H.; Rossi, F. *Langmuir* **2008**, *24*, 7251–7261.

(19) Findlay, J. W. A.; Dillard, R. F. *J. Am. Assoc. Pharm. Scientists* **2007**, *9*, E260–E266.

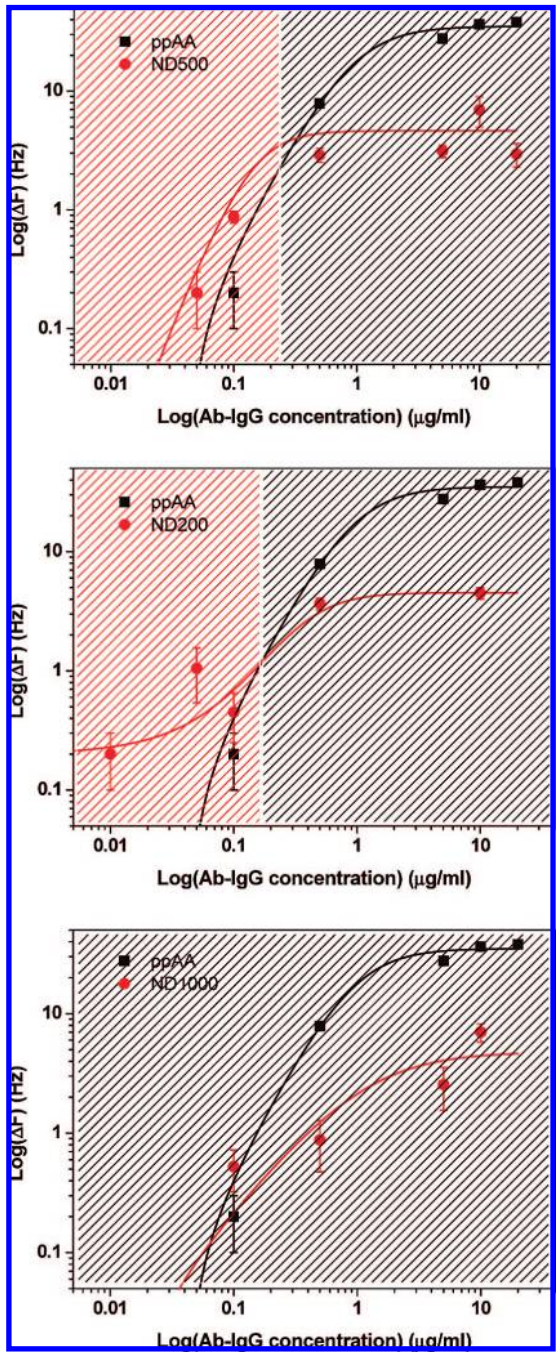

Figure 3. Dose−response curves for the flat ppAA and the nanostructured surfaces. The solid lines are the sigmoidal-shaped functions best-fitting the calibration curves. The curve for ppAA is reported in each graph for direct comparison with the nanostructured surfaces. The red- and the black-colored areas represent respectively the concentration regions where the signal from the nanostructured surface and the nonstructured surface is higher.

respect to the ppAA surface LOD. Unfortunately, further reduction of the LOD cannot be observed due to the intrinsic LOD of the QCM system.

In order to underline the positive effect in terms of the reduction of the sensor's working range observed with the nanopatterned surfaces, the fitted calibration curves for the ppAA and for the nanostrucutred surfaces have been normalized and plotted on a log-linear scale and are shown in Figure 4.

Table 2. Quality Factors for the IgG−Ab-IgG Immunosensor with the Differently Functionalized Surfaces[a]

surface	A2 (saturation) (Hz)	C_0 (μg/mL)	p	LOD (μg/mL)
ppAA	35.06 ± 0.64	0.98 ± 0.06	1.05 ± 0.21	0.5
ND200	4.52 ± 0.50	0.37 ± 0.07	3.73 ± 0.58	<0.1
ND500	5.13 ± 1.27	0.14 ± 0.02	1.23 ± 0.80	0.1
ND1000	4.79 ± 1.49	1.2 ± 1.06	1.19 ± 0.53	0.1

[a] The parameters are fitted by using eq 1.

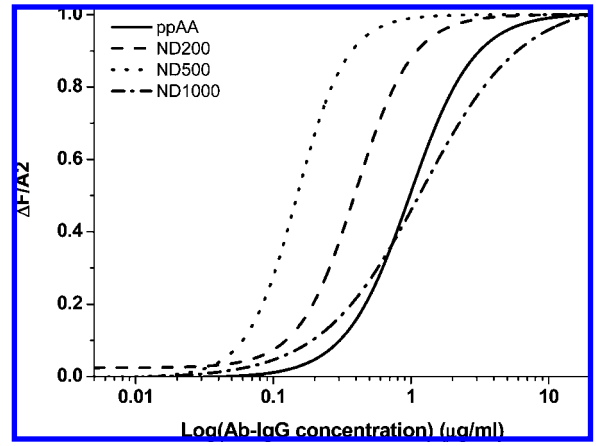

Figure 4. Normalized dose−response curves fitted with the sigmoidal-shaped function for the flat ppAA and the nanostructured surfaces plotted in log-linear scale.

It is graphically evidenced in Figure 4 that the C_0 factor for the ND500 and ND200 surfaces is shifted toward the lower concentrations with respect to the one for the ppAA surface.

The reduction of the working range and of the LOD produced by the nanostructures can be attributed to the effect of the confinement of the IgG molecules on the COOH adhesive areas. In fact, the confinement of molecules produces three principal effects:

(1) It reduces the surface mobility of the IgG molecules during the adsorption. This is reflected in a faster kinetics of adsorption compared to a nonstructured surface, as observed by QCM-D (data not shown). This means that the IgG molecules absorbing on the nanostructures have less possibility of denaturation with respect to a nonstructured surface, preventing their immunoactivity. Confinement may also have special effects on the orientation of the IgG as already shown in our previous work.

(2) The presence of the antiadhesive material between the adhesive spots reduces the steric hindrance of the IgG molecules, increasing their activity.

(3) The presence of highly adhesive areas in a nonadhesive matrix may influence the diffusion of the Ab-IgG molecules, increasing the probability of reaction with the immobilized IgG. Due to the antiadhesive separation between the active bioadhesive spots, the diffusion of the Ab-IgG molecules toward the nanostructures is similar to the radial diffusion that occurs in the case of electrochemcial species through nanoelectrodes.[20] This effect increases the availability of the immobilized IgG molecules binding sites for the interaction with their antibody.

(20) Arrigan, D. W. M. *Analyst* **2004**, *129*, 1157–1165.

CONCLUSION

We observed an evident concentration-dependent scaling effect on the reactivity of IgG molecules immobilized on nanostructured surfaces characterized by adhesive (ppAA) nanodomains separated by an antifouling (PEO-like matrix) and nonstructured ppAA surfaces.

The bioactivity of the immobilized IgG molecules was checked by monitoring the specific reaction with their antibodies. The nanopatterned surfaces demonstrate a higher antibody recognition capability for Ab-IgG concentration lower than 0.1 μg/mL with respect to the unstructured ppAA surface. Moreover, the working range of the sensor (measured by the C_0 factor) is reduced by a factor 7 on the nanopatterned surface, together with a reduction of the LOD of a factor 5 with respect to the unstructured surface.

The results obtained in this work are extremely interesting for the development of the efficiency of immunosensing devices, evidencing the capability of the nanostructured surfaces of representing universal platforms for ultrasensitive devices.

ACKNOWLEDGMENT

The authors thank Takao Sasaki for the SEM images and Simone Malfara′ and Giovanni Maselli for technical support. The work has been supported by the European Commission Joint Research Center Action "NanoBiotechnology for Health.

Received for review May 20, 2008. Accepted July 21, 2008.

AC801021Z